Acta Radiologica Open
5(1) 1–7

DOI: 10.1177/2058460116628340
arr.sagepub.com

Model-based iterative reconstruction and adaptive statistical iterative reconstruction: dose-reduced CT for detecting pancreatic calcification

Koichiro Yasaka[1], Masaki Katsura[1], Masaaki Akahane[2], Jiro Sato[1], Izuru Matsuda[3] and Kuni Ohtomo[1]

Abstract

Background: Iterative reconstruction methods have attracted attention for reducing radiation doses in computed tomography (CT).

Purpose: To investigate the detectability of pancreatic calcification using dose-reduced CT reconstructed with model-based iterative construction (MBIR) and adaptive statistical iterative reconstruction (ASIR).

Material and Methods: This prospective study approved by Institutional Review Board included 85 patients (57 men, 28 women; mean age, 69.9 years; mean body weight, 61.2 kg). Unenhanced CT was performed three times with different radiation doses (reference-dose CT [RDCT], low-dose CT [LDCT], ultralow-dose CT [ULDCT]). From RDCT, LDCT, and ULDCT, images were reconstructed with filtered-back projection (R-FBP, used for establishing reference standard), ASIR (L-ASIR), and MBIR and ASIR (UL-MBIR and UL-ASIR), respectively. A lesion (pancreatic calcification) detection test was performed by two blinded radiologists with a five-point certainty level scale.

Results: Dose-length products of RDCT, LDCT, and ULDCT were 410, 97, and 36 mGy-cm, respectively. Nine patients had pancreatic calcification. The sensitivity for detecting pancreatic calcification with UL-MBIR was high (0.67–0.89) compared to L-ASIR or UL-ASIR (0.11–0.44), and a significant difference was seen between UL-MBIR and UL-ASIR for one reader ($P = 0.014$). The area under the receiver-operating characteristic curve for UL-MBIR (0.818–0.860) was comparable to that for L-ASIR (0.696–0.844). The specificity was lower with UL-MBIR (0.79–0.92) than with L-ASIR or UL-ASIR (0.96–0.99), and a significant difference was seen for one reader ($P < 0.01$).

Conclusion: In UL-MBIR, pancreatic calcification can be detected with high sensitivity, however, we should pay attention to the slightly lower specificity.

Keywords
Abdomen/GI, computed tomography (CT), pancreas, calcifications/calculi, adults, observer performance

Date received: 17 September 2015; accepted: 1 January 2016

Introduction

Chronic pancreatitis is a progressive inflammatory disease that causes destruction of pancreatic parenchyma and replacement by fibrous tissue (1). Several factors are related to this disease, such as alcohol, smoking, hypercalcemia, pancreatic divisum, etc. (2,3). The incidence and prevalence of chronic pancreatitis are reported to be 5–12 and 20–50 per 100,000 people, respectively (4–6). Chronic pancreatitis can cause upper abdominal pain, malnutrition, and diabetes (1,2), and it is also reported to be a risk factor for

[1]Department of Radiology, Graduate School of Medicine, The University of Tokyo, Tokyo, Japan
[2]NTT Medical Center Tokyo, Tokyo, Japan
[3]Kanto Rosai Hospital, Kawasaki, Kanagawa, Japan

Corresponding author:
Koichiro Yasaka, Department of Radiology, The University of Tokyo Hospital 7-3-1 Hongo, Bunkyo-ku, Tokyo, Japan.
Email: koyasaka@gmail.com

pancreatic carcinoma (7–10). Therefore, the diagnosis of chronic pancreatitis is important.

In diagnosing chronic pancreatitis, histological methods are not commonly used, and imaging findings play an important role (2). There are several imaging findings of chronic pancreatitis, such as dilation of the pancreatic duct and atrophy of pancreatic parenchyma (11). Pancreatic calcification is also an important imaging finding. It can be detected on computed tomography (CT) without using contrast enhancement media. Its specificity in diagnosing chronic pancreatitis is reported to be 67–100% (12). The prevalence of calcifications in chronic pancreatitis varies according to the interval from the onset of symptoms: 37–59% after 8–25 years; and 80–91% after 14–36 years (11). However, there is an important issue to consider: CT carries a risk of X-ray radiation exposure.

Recently, iterative reconstruction methods such as adaptive statistical iterative reconstruction (ASIR) and model-based iterative reconstruction (MBIR) have attracted much attention for reducing radiation doses. ASIR takes into account a statistical noise model in the process of iteration and enables dose reduction compared with filtered back projection (FBP) (13–15). MBIR is a more complex and accurate procedure than ASIR. It considers not only a statistical noise model as in ASIR, but also the modeling of the system optics. MBIR enables further dose reduction without severely increasing noise and artifacts compared with ASIR (16,17). According to a recent report, MBIR is superior to FBP in depiction of the pancreatic duct (18), dilation of which can be an important imaging feature of chronic pancreatitis. However, to the best of our knowledge, there have been no reports of the detectability of pancreatic calcification using dose-reduced CT with iterative reconstruction. Because the usefulness of aggressively reduced dose CT for detecting urolithiasis was reported (19) and the chance of performing ultralow-dose CT is expected to increase, this issue should be investigated.

The purpose of the present study was to investigate the detectability of pancreatic calcification using dose-reduced CT reconstructed with MBIR, compared with ASIR.

Material and Methods

This was a prospective clinical study approved by the Institutional Review Board. Written informed consent was obtained from each patient.

Patients

The institute's Radiological Information System was checked to identify patients scheduled to undergo unenhanced abdominopelvic CT in a single tertiary care center. These patients were scheduled for unenhanced CT based on the attending physician's request (e.g. no clinical indication for using contrast, history of a previous adverse reaction to iodine contrast enhancement material, or impairment of renal function). Some patients were identical to those in previous studies that evaluated image quality and diagnostic performance for hepatic steatosis using abdominopelvic CT with iterative reconstruction. Inclusion criteria were as follows: age >50 years; non-emergent; ability to give written informed consent; and the ability to hold breath and remain still for at least 10 s. Those who could not give written informed consent, follow verbal commands for breath holding or remain still were excluded. Patients who were pregnant or trying to get pregnant were also excluded.

Each potential subject was given explanations about the objective, methods, and risks of the study. The explanation included that reference-dose CT (RDCT), low-dose CT (LDCT), and ultralow-dose CT (ULDCT) would be performed, the total radiation exposure would not exceed the standard-of-care CT in our hospital, and the diagnostic performance of RDCT might be slightly inferior to that of standard-of-care CT.

From October 2011 to December 2011, 98 consecutive eligible patients were identified. Seven refused to participate in the study, and none withdrew after signing the consent form. Consequently, 91 patients gave written informed consent. Of these patients, six were selected randomly, and their CT images were used to understand the evaluation methods. Finally, images of 85 patients (57 men, 28 women; mean age, 69.9 ± 9.0 years; mean body weight, 61.2 ± 12.2 kg) were included in the analyses. The purposes of the CT examinations were to evaluate malignancy ($n = 52$), urolithiasis ($n = 15$), abdominal aortic aneurysm ($n = 11$), and others ($n = 7$).

CT image acquisition

All CT scans were performed with a 64-row multidetector CT (Discovery CT750 HD; GE Healthcare, Waukesha, WI, USA). RDCT was immediately followed by LDCT and ULDCT. Patients were scanned in the supine position, both arms elevated, and a single breath held for each scan. The scanning parameters other than tube current were kept constant between scans: tube potential, 120 kVp; helical acquisition mode; pitch, 1.375: 1; gantry rotation time, 0.4 s; field of view, 360 mm (adjusted for patient size); and detector configuration, 64×0.625 mm. As for setting the tube current, automatic tube current modulation (Auto mA 3D; GE Healthcare) was used. We setup

the radiation exposure so that the total radiation dose of RDCT, LDCT, and ULDCT would not exceed that of standard-of-care CT performed in our hospital. Considering that the image noise is known to be inversely proportional to square root of radiation dose and that the noise index of standard-of-care CT in our hospital is 10.6 for 5 mm slice thickness, the following noise indices (for 5 mm thickness) with minimum and maximum tube currents were chosen: 12.3 (100–600 mA) for RDCT, 24.6 (25–120 mA) for LDCT, and 40.6 (10–45 mA) for ULDCT. Axial images with 0.625-mm slice thickness were reconstructed. By averaging, images with 2.5-mm slice thickness were also generated and could be referenced as necessary. For reconstructing images of FBP and ASIR, STANDARD kernel was used. From RDCT, images were reconstructed with FBP (R-FBP), and they were used as the reference standard. From LDCT and ULDCT, images were reconstructed with ASIR (L-ASIR), and ASIR and MBIR (UL-ASIR and UL-MBIR), respectively. Images of ASIR were reconstructed at 50% ASIR-FBP blending.

Radiation dose

Radiation doses were recorded according to the dose report that included the estimated CT dose index volume (CTDI vol) and the dose-length product (DLP) for each image dataset after completing the CT examination.

Image analysis

Objective image analysis was performed by a radiologist (K.Y.; 6 years of experience as a radiologist) with a commercial viewer (Centricity; GE Healthcare). A circular or ovoid region of interest (ROI) with a diameter of 1–1.5 cm was placed at the head of the pancreas. ROIs were carefully placed so that the place and size were almost identical among three images not referencing the measured results. In placing ROIs, apparent calcification was avoided. CT attenuation and standard deviation (i.e. image noise) were recorded. These measurements were performed twice and the results were averaged.

Two radiologists (J.S. and I.M., with 13 and 6 years of experience as radiologists, respectively) were included for subjective image analysis. Both had 3 and 0.5 years of experience with ASIR and MBIR. They evaluated the presence of pancreatic calcification (calcification of pancreatic parenchyma or pancreatic duct) by a five-point certainty level scale (1, no calcification; 2, calcification probably not present; 3, calcification presence equivocal; 4, calcification probably present; 5, calcification definitely present) per patient, with a commercial viewer (EV Insite; PSP Corporation, Tokyo, Japan). Images were shown with a default window setting (window width of 290 Hounsfield units [HU] and window level of 45 HU), which were allowed to change for ease of assessment. To assess intra-observer agreement, eight patients (24 image sets) were randomly selected from the 85 patients, and these 24 image sets were evaluated twice. Consequently, 279 image sets were analyzed. They were shown in a random manner. Both radiologists were blinded to patient data and image reconstruction techniques.

A consensus panel of two different radiologists (M.K. and K.Y., with 8 and 6 years of experience, respectively) independently interpreted the images of R-FBP and identified the calcifications. For establishing a reference standard, the candidate calcifications identified by the previous two radiologists (J.S. and I.M.) were taken into account. Patients with calcification in whom it was not clear whether it was located within the pancreas even by referencing images of R-FBP were excluded. The location (pancreatic head, Ph; pancreatic body, Pb; pancreatic tail, Pt) and number of pancreatic calcifications were recorded. The size of the largest calcification was also measured. For patients who were falsely evaluated as having pancreatic calcification on UL-MBIR by either of two radiologists (J.S. or I.M.), the presence of mistakable calcifications around the pancreatic parenchyma was also assessed.

Statistical analysis

Statistical analyses were performed with SPSS Statistics version 21 (IBM SPSS Japan, Tokyo, Japan). For analyzing CT attenuation and image noise, the paired *t*-test was used. Inter-observer and intra-observer agreements were calculated with Cohen's weighted kappa analysis. The following kappa values were used to indicate agreement: 0–0.20, poor agreement; 0.21–0.40, fair agreement; 0.41–0.60, moderate agreement; 0.61–0.80, good agreement; and 0.81–1.00, excellent agreement. Sensitivity, specificity, accuracy, positive predictive value (PPV), and negative predictive value (NPV) for detecting pancreatic calcification were calculated. Scores of 5 and 4 were defined as positive. Sensitivity, specificity, and accuracy were compared between images with McNemar's test. Receiver operating characteristic (ROC) analysis was performed with ROCKIT (The University of Chicago, Chicago, IL, USA). Areas under the curve (AUC) were calculated and compared.

For comparing multiple groups (UL-MBIR and L-ASIR or UL-MBIR and UL-ASIR), the Bonferroni correction was applied, and $P < 0.025$ was considered to indicate a significant difference.

Results

The CTDI vol and DLP of each scan (RDCT, LDCT, and ULDCT) were 7.99 ± 2.90, 1.89 ± 0.58, and 0.70 ± 0.22 mGy and 410 ± 166, 97 ± 34, and 36 ± 13 mGy-cm, respectively.

The objective image noise was significantly lower with UL-MBIR (18.9) than with L-ASIR (image noise, 46.2; $P < 0.001$) and UL-ASIR (image noise, 81.5; $P < 0.001$). The CT attenuation of the pancreatic head was 30.1, 31.2, and 32.4 HU with UL-MBIR, L-ASIR, and UL-ASIR, respectively. There was no significant difference between UL-MBIR and L-ASIR ($P = 0.051$). The CT attenuation of the pancreatic head was significantly higher with UL-ASIR than with UL-MBIR ($P < 0.001$).

Nine patients had pancreatic calcification (Fig. 1). The location of the calcification was clear in all cases. The details of pancreatic calcifications are described in Table 1. The actual certainty score for the presence of pancreatic calcification by each reader is summarized in Table 2. With UL-ASIR, many cases were evaluated as 3 (presence equivocal) by both readers. The inter-observer agreement was fair ($\kappa = 0.381$), and the intra-observer agreement was fair to moderate ($\kappa = 0.264$ for reader 1 and $\kappa = 0.418$ for reader 2).

The sensitivity, specificity, accuracy, PPV, and NPV are shown in Table 3. The sensitivity of both readers tended to be high with UL-MBIR (0.67–0.89)

Table 1. Characteristics of pancreatic calcifications.

Patient	Calcifications (n)	Size of maximum calcification (mm)	Distribution of calcifications
1	>10	≤6	Ph, Pb, and Pt
2	2	≤4	Ph and Pb
3	>10	≤4	Ph, Pb, and Pt
4	2	≤3	Pb and Pt
5	3	≤4	Ph and Pb
6	5	≤5	Ph and Pb
7	4	≤3	Pb and Pt
8	2	≤3	Pb
9	1	3	Ph

Pb, pancreatic body; Ph, pancreatic head; Pt, pancreatic tail.

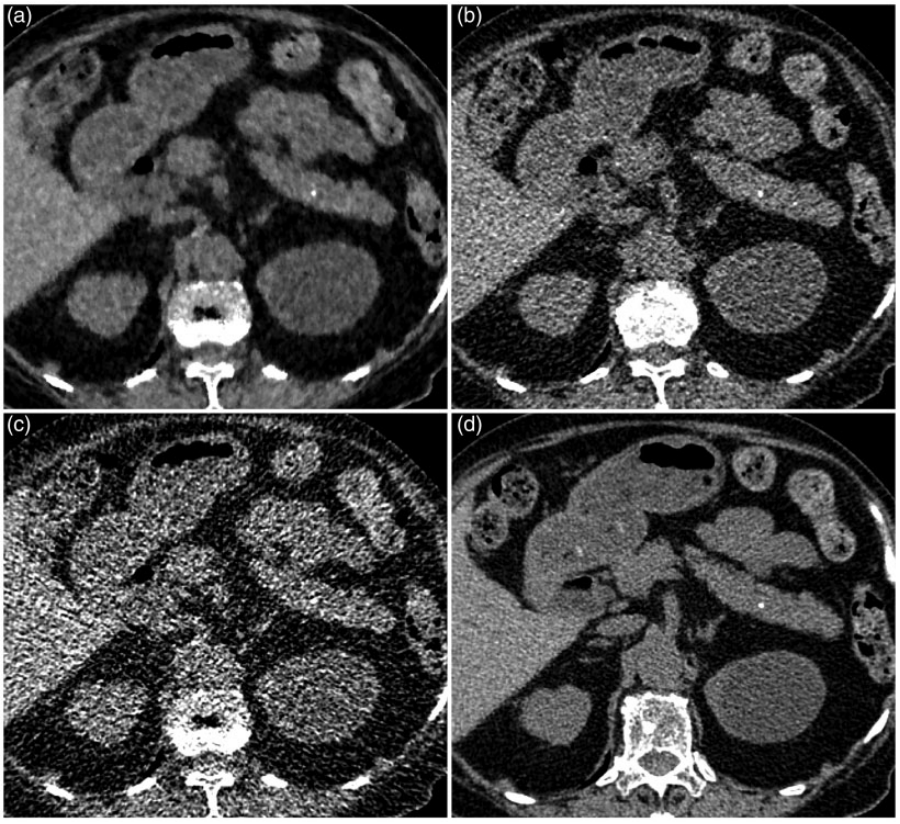

Fig. 1. Axial unenhanced CT images of UL-MBIR (a), L-ASIR (b), UL-ASIR (c), and R-FBP (d) of an 82-year-old woman weighing 44 kg. Pancreatic calcification (3 mm diameter) is clearly depicted on UL-MBIR. On UL-MBIR/L-ASIR/UL-ASIR, it was evaluated as 4 (calcification probably present)/2 (calcification probably not present)/3 (calcification presence equivocal) by reader 1 and 4/3/3 by reader 2.

Table 2. Actual evaluation scores for each reconstruction method.

Pancreatic calcification	UL-MBIR	L-ASIR	UL-ASIR
Reader 1			
Positive (5/4/3/2/1)	2/6/0/1/0	2/1/1/5/0	1/2/4/3/0
Negative (5/4/3/2/1)	0/16/8/48/4	0/3/7/60/6	0/0/41/31/3
Reader 2			
Positive (5/4/3/2/1)	2/4/3/0/0	3/1/4/1/0	1/0/8/0/0
Negative (5/4/3/2/1)	2/4/59/10/1	0/1/29/29/17	1/2/67/5/1

Scores indicate the followings: 5, calcification definitely present; 4, calcification probably present; 3, calcification presence equivocal; 2, calcification probably not present; 1, no calcification.

Table 3. Sensitivity, specificity, accuracy, PPV, and NPV for detecting pancreatic calcification.

	Values			Comparison (*P* value)	
	UL-MBIR	L-ASIR	UL-ASIR	UL-MBIR vs. L-ASIR	UL-MBIR vs. UL-ASIR
Reader 1					
Sensitivity	0.89 (8/9)	0.33 (3/9)	0.22 (2/9)	0.025	0.014*
Specificity	0.79 (60/76)	0.96 (73/76)	0.99 (75/76)	0.002*	<0.001*
Accuracy	0.80 (68/85)	0.89 (76/85)	0.91 (77/85)	0.088	0.061
PPV	0.33 (8/24)	0.50 (3/6)	0.67 (2/3)	N/A	N/A
NPV	0.98 (60/61)	0.92 (73/79)	0.91 (75/82)	N/A	N/A
Reader 2					
Sensitivity	0.67 (6/9)	0.44 (4/9)	0.11 (1/9)	0.157	0.025
Specificity	0.92 (70/76)	0.99 (75/76)	0.96 (73/76)	0.059	0.180
Accuracy	0.89 (76/85)	0.93 (79/85)	0.87 (74/85)	0.317	0.527
PPV	0.50 (6/12)	0.80 (4/5)	0.25 (1/4)	N/A	N/A
NPV	0.96 (70/73)	0.94 (75/80)	0.90 (73/81)	N/A	N/A

For comparison, McNemar's test was used.
*$P < 0.025$.
N/A, not applicable; NPV, negative predictive value; PPV, positive predictive value.

compared to L-ASIR and UL-ASIR (0.11–0.44), and a significant difference was seen between UL-MBIR and UL-ASIR for reader 1 ($P = 0.014$). The specificity of both readers tended to be a little lower with UL-MBIR (0.79–0.92) than with L-ASIR and UL-ASIR (0.96–0.99), and a significant difference was seen for reader 1 ($P < 0.01$). With UL-MBIR, the numbers of false-positive cases were 16 and 6 for reader 1 and reader 2, respectively. Among these patients, calcification near pancreatic tissue, such as the kidney or splenic arterial wall, was seen in two and four patients for readers 1 and 2, respectively (Fig. 2). The results of ROC analysis are summarized in Table 4. The AUC with UL-MBIR (0.818–0.860) was comparable to that with L-ASIR (0.696–0.844) and had a tendency to be superior to that with UL-ASIR (0.572–0.621), though no significant difference was seen ($P > 0.03$).

Discussion

CT is a useful modality for detecting pancreatic calcification, which is an important imaging feature of chronic pancreatitis. From our study it has become evident that MBIR enables further dose reduction compared to ASIR without compromising sensitivity for detecting pancreatic calcification. However, we should pay attentions to the slightly low specificity with MBIR in ultralow-dose level CT. Because the chance of performing ultralow-dose CT is expected to increase in the near future, especially for detecting urolithiasis (19), our study results would benefit radiologists in evaluations of incidentally found pancreatic lesions suspicious of pancreatic calcifications.

The sensitivity for detecting pancreatic calcification with UL-MBIR tended to be superior to that with L-ASIR and UL-ASIR. Remarkably reduced image noise with UL-MBIR may have resulted in a clearer depiction of pancreatic calcifications. However, the number of patients who had pancreatic calcification was low, and a significant difference was seen for only one reader.

The specificity with UL-MBIR was lower than with L-ASIR or UL-ASIR in this study. There might be two reasons for this phenomenon. One is that remarkably reduced image noise resulted in clearer depiction of calcification of the splenic or renal arterial wall, but it was not enough to discriminate pancreatic parenchyma from arterial lumen. Because these mistakable calcifications near pancreatic tissue were not found for some patients, there might be another reason. The other possible reason is that the unfamiliar imaging texture of a blotchy pixelated appearance, which is uniquely seen in images reconstructed with MBIR (17), might also have resulted in false-positive findings. According to Li et al., the shape of noise power spectrum of MBIR is strongly dose-dependent while that of FBP is dose-independent (20). Lower dose leads to noise texture of a relatively coarse graininess with MBIR, which might be related to blotchy pixelated appearance. Some high attenuation area with coarse grain like shape due to dose reduction with MBIR might have been mistakable as coarse faint calcifications of pancreas.

There were several limitations in the present study. First, the reconstruction algorithms of MBIR and ASIR are unique to GE Healthcare, and the study results might not be applicable to other iterative reconstruction algorithms from other vendors. Second, the body size of subjects (mean body weight, 61.2 kg) was

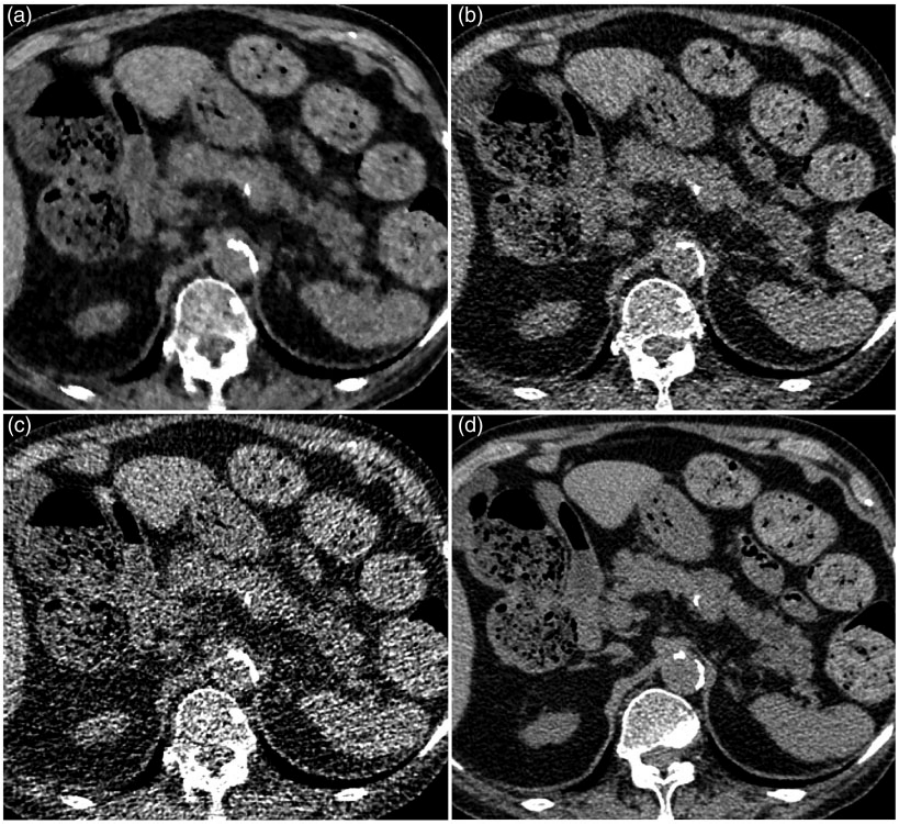

Fig. 2. Axial unenhanced CT images of UL-MBIR (a), L-ASIR (b), UL-ASIR (c), and R-FBP (d) of an 81-year-old woman weighing 60 kg. A calcification of the splenic arterial wall is seen on R-FBP (d), but this patient has no pancreatic calcification. The evaluation score for this patient on UL-MBIR/L-ASIR/UL-ASIR was 2 (calcification probably not present)/2/2 by reader 1 and 4 (calcification probably present)/3 (calcification presence equivocal)/3 by reader 2. It is possible that a calcification of the splenic arterial wall has been misdiagnosed as pancreatic calcification on UL-MBIR (a) by reader 2.

Table 4. Receiver operating characteristic analysis results for detecting pancreatic calcification.

	Area under the curve			Comparison (*P* value)	
	UL-MBIR	L-ASIR	UL-ASIR	UL-MBIR vs. L-ASIR	UL-MBIR vs. UL-ASIR
Reader 1	0.860	0.696	0.621	0.059	0.030
Reader 2	0.818	0.844	0.572	0.530	0.195

No significant differences are seen.

generally small. The diagnostic performance in extremely large patients should be investigated in the future. Third, because of the characteristic image appearance, it was quite difficult to blind reconstruction methods, but the images were presented in a random manner. Finally, we did not obtain the definitive diagnosis of chronic pancreatitis. However, according to the previous report, as many as 68% of patients who had pancreatic calcifications were diagnosed as chronic pancreatitis, and the other disease entities included pancreatic neoplasms which is also clinically important (12). Finally, though urolithiasis also shows high CT attenuation, our study results do not necessarily apply for evaluations of it.

In conclusion, pancreatic calcification could be detected with high sensitivity with ULDCT reconstructed with MBIR compared with LDCT or ULDCT reconstructed with ASIR. However, caution is needed due to the slight increase in false-positive findings.

Declaration of conflicting interests

The authors declared no potential conflicts of interest with respect to the research, authorship, and/or publication of this article.

Funding

This research received no specific grant from any funding agency in the public, commercial, or not-for-profit sectors.

References

1. Braganza JM, Lee SH, McCloy RF, et al. Chronic pancreatitis. Lancet 2011;377:1184–1197.
2. Etemad B, Whitcomb DC. Chronic pancreatitis: diagnosis, classification, and new genetic developments. Gastroenterology 2001;120:682–707.
3. Gonoi W, Akai H, Hagiwara K, et al. Pancreas divisum as a predisposing factor for chronic and recurrent idiopathic pancreatitis: initial in vivo survey. Gut 2011;60: 1103–1108.
4. Yadav D, Lowenfels AB. The epidemiology of pancreatitis and pancreatic cancer. Gastroenterology 2013;144: 1252–1261.
5. Jupp J, Fine D, Johnson CD. The epidemiology and socioeconomic impact of chronic pancreatitis. Best Pract Res Clin Gastroenterol 2010;24:219–231.
6. Liao Z, Jin G, Cai D, et al. Guidelines: diagnosis and therapy for chronic pancreatitis. J Interv Gastroenterol 2013;3:133–136.
7. Lowenfels AB, Maisonneuve P, Cavallini G, et al. Pancreatitis and the risk of pancreatic cancer. International Pancreatitis Study Group. N Engl J Med 1993;328:1433–1437.
8. Ekbom A, McLaughlin JK, Karlsson BM, et al. Pancreatitis and pancreatic cancer: a population-based study. J Natl Cancer Inst 1994;86:625–627.
9. Bansal P, Sonnenberg A. Pancreatitis is a risk factor for pancreatic cancer. Gastroenterology 1995;109:247–251.
10. Fernandez E, La Vecchia C, Porta M, et al. Pancreatitis and the risk of pancreatic cancer. Pancreas 1995;11: 185–189.
11. DiMagno MJ, DiMagno EP. Chronic pancreatitis. Curr Opin Gastroenterol 2010;26:490–498.
12. Campisi A, Brancatelli G, Vullierme MP, et al. Are pancreatic calcifications specific for the diagnosis of chronic pancreatitis? A multidetector-row CT analysis. Clin Radiol 2009;64:903–911.
13. Prakash P, Kalra MK, Kambadakone AK, et al. Reducing abdominal CT radiation dose with adaptive statistical iterative reconstruction technique. Invest Radiol 2010;45:202–210.
14. Sagara Y, Hara AK, Pavlicek W, et al. Abdominal CT: comparison of low-dose CT with adaptive statistical iterative reconstruction and routine-dose CT with filtered back projection in 53 patients. Am J Roentgenol 2010; 195:713–719.
15. Singh S, Kalra MK, Hsieh J, et al. Abdominal CT: comparison of adaptive statistical iterative and filtered back projection reconstruction techniques. Radiology 2010; 257:373–383.
16. Katsura M, Matsuda I, Akahane M, et al. Model-based iterative reconstruction technique for radiation dose reduction in chest CT: comparison with the adaptive statistical iterative reconstruction technique. Eur Radiol 2012;22:1613–1623.
17. Yasaka K, Katsura M, Akahane M, et al. Model-based iterative reconstruction for reduction of radiation dose in abdominopelvic CT: comparison to adaptive statistical iterative reconstruction. Springerplus 2013;2:209.
18. Lin XZ, Machida H, Tanaka I, et al. CT of the pancreas: comparison of image quality and pancreatic duct depiction among model-based iterative, adaptive statistical iterative, and filtered back projection reconstruction techniques. Abdom Imaging 2014;39:497–505.
19. Glazer DI, Maturen KE, Cohan RH, et al. Assessment of 1 mSv urinary tract stone CT with model-based iterative reconstruction. Am J Roentgenol 2014;203:1230–1235.
20. Li K, Tang J, Chen GH. Statistical model based iterative reconstruction (MBIR) in clinical CT systems: experimental assessment of noise performance. Med Phys 2014;41:041906.